WITHDRAWN: Rhizosphere Microbiome is Associated with Yield and Medical Value of the Perennial Panax Notoginseng

Guangfei Wei
China Academy of Chinese Medical Sciences
Mengzhi Li
China Academy of Chinese Medical Sciences
Guozhuang Zhang
China Academy of Chinese Medical Sciences
Zhongjian Chen
Wenshan University
Fugang Wei
Wenshan Miaoxiang Notoginseng Technology, Co., Ltd
Shuo Jiao
Northwest Agriculture and Forestry University
Jun Qian
China Academy of Chinese Medical Sciences
Yong Wang
Wenshan University
Xiangxiao Meng
China Academy of Chinese Medical Sciences
Yuqi Yu
Wenshan Miaoxiang Notoginseng Technology, Co., Ltd.
Linlin Dong
lldong@icmm.ac.cn

Institute of Chinese Materia Medica, China Academy of Chinese Medical Sciences
https://orcid.org/0000-0002-2054-8749
Shilin Chen
Institute of Chinese Materia Medica, China Academy of Chinese Medical Sciences

Research

Keywords: Panax notoginseng, rhizosphere microbiomes, developmental stages, belowground biomass, saponin contents

Posted Date: July 16th, 2020

DOI: https://doi.org/10.21203/rs.3.rs-41495/v1

EDITORIAL NOTE:

The full text of this preprint has been withdrawn by the authors while they make corrections to the work. Therefore, the authors do not wish this work to be cited as a reference. Questions should be directed to the corresponding author.

Abstract

Background: Rhizosphere microbiome play important roles in promoting plant growth. However, it is not well understood how rhizosphere microbiome were driven by medical plants during growth stages and whether they contribute the accumulation of medical values. *Panax notoginseng* is a perennial medicinal plant, which belowground biomass and saponin contents are the important indicators of its value. Here, we use high-throughput sequencing method to study the temporal dynamics of perennial *P. notoginseng* rhizosphere microbiomes and the relationship between the indicators and core rhizosphere microbiomes.

Results: The results show that the diversity, composition and network structures of the bacterial and fungal communities are mainly driven by the developmental stages. And succession characteristics of bacterial and fungal diversity show similar parabolic patterns during the developmental stages. Enrichment and depletion of the bacterial and fungal communities are active at the 3-year root growth (3YR) stage. From samples collected at a large-spatial *P. notoginseng* production area at the 3YR stage, we obtained 639 bacterial and 310 fungal core operational taxonomic units (OTUs). Analysis of the data indicate that the microbiome diversity is related to the belowground biomass and total saponin contents. Some genera, such as *Pseudomonas*, *Massilia*, *Sphingobium*, and *Phoma* are positively correlated to the belowground biomass, and genera likely *Staphylotrichum*, *Chaetosphaeria*, *and Podospora* are positively correlated with total saponin contents. Additionally, we identified 36 microbial functions involving in plant-microbe and microbe-microbe interactions, nutrition acquisition, and disease resistance. They are related to belowground biomass and saponin contents.

Conclusions: In short, this study provides a detailed and systematic survey of rhizosphere microbiome in *P. notoginseng* and reveals that *P. notoginseng* rhizosphere microbiomes are largely driven by the developmental stages, while the core microbiomes are related to the belowground biomass and saponins contents of the plant. The finding may enhance our understanding of the interaction between microbes and perennial plants and improve our ability to manage root microbiota for sustainable production of the herb medicine.

Background

Rhizosphere microbiomes have been recognized as important for plant nutrition, growth [1], and resistance against pathogen invasion [2]. Plants could affect the diversity, composition, structure, and function of the rhizosphere microbiome [3, 4]. Meanwhile, plant growth stages also affect the microbial community [5]. Diversity and composition of rhizosphere bacterial communities associated with *Arabidopsis thaliana* at the seedling stage are significantly different from other stages (vegetative, bolting, and flowering) [6]. Evidence shows that soybeans in the vegetative stage impact on the structures of bacterial communities, which may be continuously altered throughout their late growth stages [7]. Variations in the composition of rhizodeposition allow plants to shape rhizosphere microbial communities for their benefit, which is a result of selection power of the plant [8]. Therefore,

understanding the succession in rhizosphere during plant growth stages is of great significance for improving agricultural practices [9].

Medicinal plants are essential for improving human health, approximately 75% of the population in developing countries mainly rely on herb-based medicines for health care around the world [10]. Many medicinal plants are perennial, including transitions from seedling, flowering, to aging annually. In case of *Panax ginseng*, recent study indicates that the rhizosphere bacterial diversity decreases and fungal diversity increases at the root growth stage compared to vegetative, flowering and fruiting stages [11]. Major active components of medicinal plants are the secondary metabolites, whose contents are influenced by many environmental factors, such as climatic and edaphic factors [12, 13]. Nevertheless, rhizosphere microbiomes directly impact the metabolome of host plants, thus influencing the efficacy of herbal medicines [14]. When *Matricaria chamomilla* grow in different locations, the contents of secondary metabolites are different and depend on microbe composition [15]. Therefore, the succession characteristics of rhizosphere microbiome during the developmental stages of perennial medicinal plants could mediate the accumulation of secondary metabolism. However, it is not well understood to what extent a perennial medicinal plant during development stages can select a constant and beneficial rhizosphere community. It is of importance for starting a rigorous investigating the interaction and association between rhizosphere microbes and secondary metabolism which traits is crucial for medicinal plant breeding.

Panax notoginseng is an important medicinal plant known as “Nanguo Shencao (Miracle Plant from South China)”, and used as the main raw material in Yunnan Baiyao and Xuesaitong due to its blood-invigorating effects [10, 16]. The therapeutic effects of *P. notoginseng* are mostly attributed to the plant’s bioactive saponin constituents, including notoginsenoside R1 and ginsenosides [17, 18]. *P. notoginseng* is a typical perennial plant mainly cultivated in the southwest of China [19]. As a perennial plant, it has vegetative, reproductive and root growth stages annually. It has been found that continuously cropping has reduced the number of rhizobacteria and fungal diversity [20, 21]. However, it is unclear how rhizosphere microbial community assembles during annual growth stages. After application of biofertilizer (*Burkholderia* and *Rhizobium*), *Panax ginseng* yield was enhanced by 17.0-19.1% and ginsenosides (Rg1 and Rb1) contents were improved [22]. These results indicate that core rhizosphere microbes may interact with *Panax* plants to regulate their secondary metabolism. Typically, *P. notoginseng* has a 3-year-long crop cycle before harvest [23]. Therefore, it is valuable to study the relationship between the core rhizosphere microbiomes and the saponin contens at the harvest stage. This information relates to the content of *P. notoginseng* saponins and may help to use beneficial microbes to improve the quality and yield of the herb in the future.

We hypothesize that rhizosphere microbiomes are driven by developmental stages and core rhizosphere microbiomes are associated with the quality of *P. notoginseng* at the harvest stage. Here we utilize amplicon and metagenomic sequencing to analyze the profiles of diversity, composition, and potential functions of rhizosphere microbiomes during different development stages of *P. notoginseng*. Specifically, we: (i) characterize the succession characteristics of rhizosphere microbiome in response to

the development stages; (ii) identify the core microbiome and function related to the quality of *P. notoginseng* at the harvest stage.

Materials And Methods

Experimental sites and collection of rhizosphere soil

Developmental stages sampling experiment

To study the temporal dynamics of microbiomes, rhizosphere soils of *P. notoginseng* were collected at five fields in Pingba (23°14'N, 104°5'E, 1767 m), Yanshan (23°34'N, 104°19'E, 1554 m) and Qiubei (23°49' N, 104°06'E, 1631 m) in Yunnan Province of China during two years growth from February 2016 to October 2017 (Fig. 1). Briefly, one-year-old seedlings were transplanted into each field and then cultivated in strict accordance with the Good Agricultural Practices [24, 25]. Every field had three separate, 1.4×8.0 m^2 plots as replicates. Before transplanting, ten soil samples were collected from random locations in each plot and combined to generate one bulk soils (BL). Then, rhizosphere soil samples were collected at one of the three developmental stages of *P. notoginseng* in each year: (1) vegetative (V, May); (2) flowering (F, Jul), (3) root growth (R, Oct), namely 2-year V (2YV), 2-year F (2YF), 2-year R (2YR), 3-year V (3YV), 3-year F (3YF), and 3-year R (3YR). At each sampling time, ten randomly selected healthy plants were removed from each plot, and mixed to generate one rhizosphere sample [26]. Thus, a total of 105 samples comprising 90 rhizosphere soil samples at six developmental stages and 15 bulk soil samples in five fields were obtained, sieved (2 mm) and stored at -80 ^{o}C for DNA extraction.

Spatial sampling experiment at the harvest stage

The belowground biomass and contents of saponins, the most important medicinal components of *P. notoginseng*, accumulate rapidly at the harvest stage (3YR), an active period of interaction between rhizosphere microbes and plants. To explore the potential contribution of core bacterial and fungal communities to the accumulation of belowground biomass and saponins contents of *P. notoginseng*, we also conducted a larger spatial scale sampling at the harvest stage in October 2017 across Yunnan and Guangxi provinces, the main production bases of *P. notoginseng*. Twenty-six sites extending from 22°2'N to 25°42'N and 100°6'E to 106°30'E were selected (Fig. 1 and Additional file 2). Three 1.4×8.0 m^2 plots were sampled as replicates at each site. Ten healthy plants were randomly collected from each plot, with rhizosphere soil being combined and processed as described above. Besides, corresponding root samples were carefully washed to root biomass and medical value measurements as described below. Totally, 78 rhizosphere soil samples and *P. notoginseng* roots were obtained. All soil samples were homogenized, sieved (2 mm) and stored at -80 ^{o}C for DNA extraction.

Analysis of edaphic and climatic factors

Edaphic factors, namely soil pH, organic matter (OM), available phosphate (AP), available potassium (AK), and total nitrogen (TN) of soil samples from developmental stage experiment were measured using

standard test methods2[27]. For the spatial sampling experiment at the harvest stage, edaphic factors were also tested 2Climatic factors (MMT: Month mean temperature; MAP: Mean annual precipitation; MAT: Mean annual temperature) were acquired from the Worldclim database (www.worldclim.org/) using a geographic information system according to the longitude and latitude values of the collected samples (ArcGIS version 2.0).

DNA extraction and amplicon sequencing

DNA was extracted from soil samples using the FastDNA SPIN Kit for Soil (MoBio Laboratories, Inc., USA). Amplification and purification were performed as previously described (Additional file 1: Table S1) [28]. Sequencing was performed on the Illumina MiSeq PE 250 platform (Shanghai Biozeron Co., Ltd., China). Obtained paired-end sequences were demultiplexed and filtered using QIIME2 [29]. Then, chimeric sequences were removed using the USEARCH tool on the basis of UCHIME [30]. Sequences were split into operational taxonomic units (OTUs) with a 97% similarity level using the UPARSE pipeline afterwards [30]. Representative sequences of OTUs were assigned to taxonomic lineages using the RDP classifier against the SILVA database (release 132) [31] for bacteria and UNITE database (release 7.1) for fungi [32]. OTUs that have less than two reads or fail to be aligned to the database (i.e. Unclassified) were removed from datasets before further analysis. Finally, 16033 bacterial OTUs and 5147 fungal OTUs were obtained in the developmental stages experiment, while 42988 bacterial and 12796 fungal OTUs were identified in the spatial sampling experiment.

Metagenomics sequencing

To explore the response of functions to the quality of *P. notoginseng*, soil samples from nine sites (i.e., Masupo Village, Yunnan Province [MLPY]; Napopohe Village, Guangxi Province [NPPH]; Daheishan Village, Yunnan Province (no pesticide residues) [DHSW]; Xichou village 2, Yunnan Province [XC2]; Daheishan Village 3, Yunnan Province [DHS3]; Maguan Village, Yunnan Province [MG]; Laosaiyi Village, Province [LSY]; Guishan Village, Yunnan Province [GS]; and Zhiguoshan Village, Yunnan Province [ZGS]) containing a wide variety of total saponin contents (ranging from 4.48% to 11.05%) were selected for shotgun metagenomic sequencing analysis. Metagenomic libraries were constructed using a TruSeq^{TM} DNA PCR-free Sample Prep Kit (Illumina, USA) according to the manufacturer's instructions [33]. The metagenomic libraries were sequenced on a HiSeq 2500 sequencer (Illumina, USA), and 150 bp paired-end reads were generated.

Determination of belowground biomass and saponin contents in *P. notoginseng*

After washing, root samples collected in the second experiment were weighed to obtain belowground biomass. The saponin contents of the *P. notoginseng* roots were analyzed using HPLC (Agilent 1260) analysis according to previous study [34].

Data analysis

Changes in microbiome composition and diversity during growth stages

OTU richness and Shannon index were calculated to estimate the α-diversity of bacterial and fungal communities based on rarefied sequences number using the rrarefy and diversity functions in “vegan” package in R [35, 36]. Linear least-square regression analyses with second-order term were performed to fit α-diversities to developmental stages using “lm” function. Non-parametric Kruskal-Wallis method was used to further test the differences of α-diversities between different growth stages, followed by Nemenyi test for multiple comparisons using “PMCMR” package [37]. Redundancy analysis (RDA) was performed to assess the influence of developmental stages and environmental factors on bacterial and fungal communities using rda function in “vegan” package [36]. Then constrained analysis of principal coordinate (CAP) was conducted to visualize the succession of bacterial and fungal communities based on Bray-Curtis dissimilarities using capscale and cmdscale functions in “vegan” package [38, 39]. Permutational multivariate analysis of variance (PERMANOVA) was carried out to determine effect size and significance of developmental stages on microbial compositions using adonis function in “vegan” package [36]. Differentially abundant taxa among microbial communities obtained from different stages were estimated by fitting a negative binomial generalized linear model in “edgeR” package [40]. Briefly, the calcNormFactors function was applied to normalize library size based on trimmed mean of M values method. Then the common and tagwise dispersions were obtained using the estimateDisp function with a design matrix. The glmFit function was performed to fit a generalized linear model with a negative binomial distribution, and differential abundant OTUs were tested using likelihood ratio test (glmLRT function); *P* values were further corrected using “BH” method [41].

Network analysis of microbiomes at different developmental stages

To evaluate the potential variation in interactions among microbial taxa as plant growth, core microbiomes in the samples of each developmental stage were identified to construct association networks following two criteria as previous described: the top 10% abundant OTUs, and the OTUs present in more than 85% and 60% samples for bacteria and fungi, respectively [42]. The compositional robust method, SPIEC-EASI (SParse InversE Covariance Estimation for Ecological ASsociation Inference), was adapted to construct association networks using the selected bacterial and fungal core OTUs [43]. All networks were constructed using the SpiecEasi package (v 1.0.7). The neighborhood selection procedure (MB) was used to infer the optimal sparseness based on the Stability Approach to Regularization Selection (StARs) with the variability threshold of 0.05 [44]. Networks were generated and analyzed using the “igraph” package [45]. A series of metrics were calculated to characterize the topological attributes of nodes and networks, including average path length, modularity, degree, betweenness centrality, and closeness centrality. The fast greedy method was applied to detect subgroups in the networks and the modularity was calculated as criterion of the division using the cluster_fast_greey and modularity functions in “igraph” package [46]. The distance between different networks was calculated on the basis of the graphlet degree distribution (GDD) [47]. Multidimensional scaling (MDS) was performed to visualize the distances between networks using cmdscale function in “vegan” package [36]. The robustness of different networks to random and targeted “attack” (node removals) were further assessed

using natural connectivity as the measure of graph stability [48]. The random removal of nodes (*n*=30 repetitions) evaluated the baseline robustness of the network. And targeted “attack” was performed following two strategies, in which nodes were removed in decreasing order of their betweenness or degree. The calculation of natural connectivity, “attack” robustness was performed using customized R script.

Core microbiomes in the spatial sampling dataset

For the spatial sampling dataset, variable clustering was conducted to filter environmental factors to reduce collinearity effects among environmental variables using the “Hmisc” package []. Core bacterial and fungal OTUs were selected based on two criteria as described above. To explore the potential correlation between productive characters of *P. notoginseng* and core microbiomes, random forest (RF) analysis was performed using “randomForest” and “rfPermute” packages [50]. Bacterial and fungal compositions were represented by two axes of NMDS analysis on the core microbiomes [51, 52]. Multivariate regression model and variance decomposition analysis were conducted to validate the results of RF analysis. Linear least-square regression analyses were conducted to assess the relationship between OTU richness of core microbiomes and the productive characters of *P. notoginseng*. Mantel test was conducted to estimate the correlation between β-diversity of core microbiomes and important indicators of medical value (i.e. belowground biomass and saponin contents) based on Bray-Curtis distance of microbiomes and Euclidean distance of indicators using mantel function in “vegan” package [36]. RF analysis was further performed to identify microbial taxa at genus level which potentially contribute to belowground biomass and total saponin contents. The numbers of marker genera were selected based on 20-fold cross-validation using rfcv function in “randomForest” package [50].

Metagenomics analysis

The raw reads from metagenome sequencing were used to generate clean reads by removing adaptor sequences, trimming, and removing low-quality reads (reads with an N base threshold of 10 and a minimum quality threshold of 20) at Biozeron, Shanghai, China. The clean reads were further trimmed using Sickle software, and trimmed reads shorter than 80 bp were discarded [53]. To identify and remove host-originated reads, the trimmed reads were mapped to *P. notoginseng* genomes using Bowtie 2 [54]. The Q20%, Q30%, and GC% variation ranges were 96.82-97.89, 91.10-93.42, and 58.03-60.94, respectively (Additional file 1: Table S2). The N50 and N90 values ranged from 778-1,297 bp to 543-593 bp, respectively, and the max contigs ranged from 67,400 to 1,151,948 bp (Additional file 1: Table S3). The metagenes were predicted using MetaProdigal (http://prodigal.ornl.gov/). Non-redundant metagenes (unigenes) were obtained using CD-HIT with an identity cut-off of 95% and a coverage cut-off of 90% (http://www.bioinformatics.org/cd-hit/) [55]. To obtain functional information for the unigenes, the protein sequences against the KO database were blasted using DIAMOND, and corresponding KEGG pathways as well as abundance were calculated against KEGG databases (release 93.0) using MinPath [56].

Structural equation model analysis

Structural equation model (SEM) was performed to further validate the casual relations among biotic and abiotic factors in the two datasets using “lavaan” package in *R*, respectively [57]. The axes of principal component analysis based on scaled variables represented edaphic factors, and axes of principal coordinate analysis based on Bray-Curtis dissimilarities were the representative of variations in microbial communities. For each dataset, group SEM were conducted to fix path coefficients among environmental factors and host factors, but keep coefficients free for paths associated with bacteria and fungi. Goodness of fit of two models were assessed using chi-square statistics and root-mean-square error of approximation (RMSEA).

Results

Diversity and composition of rhizosphere microbiomes driven by *P. notoginseng* developmental stages

Succession characteristics of α-bacterial and fungal diversity were similar during the developmental stages of *P. notoginseng* based on the values of richness and Shannon indices (Fig. 2a and 2b). Linear least-square regression with second-order term shows that the α-diversities of bacteria and fungi are parabolas with plant growth (Richness: R^2=0.75, P<0.001 for bacteria; R^2=0.52, P<0.001 for fungi. Shannon indices: R^2=0.71, P<0.001 for bacteria; R^2=0.40, P<0.001 for fungi). Compared to bulk soils (BL), values of *P. notoginseng* for both rhizosphere bacterial and fungal communities increase significantly. During the growth of *P. notoginseng*, bacterial α-diversities increase gradually in soils from 2-year-vegetative (2YV) stage to 2-year-root growth (2YR) stage. Nevertheless, the α-diversities of fungal communities peak in the 2YV stage, then fluctuate mildly until 3YF stage. Interestingly, compared to 3-year flowering (3YF) stage, the richness and Shannon indices in soil bacterial and fungal communities at the 3-year-root growth (3YR) stage are remarkably reduced. These results indicate that the α-diversity in microbial communities is shaped by the developmental stage, and dynamic succession characteristics in bacterial and fungal communities are similar.

We used redundancy analysis (RDA) to preliminarily characterize the most influential factors to the variance of microbial communities at the developmental stages (Fig. 2c and Additional file 1: Table S4). Permutational multivariate analysis of variance (PERMANOVA) based on Bray-Curtis dissimilarities revealed that developmental stages significantly drove the variation within the bacterial (R^2=37.19%, P<0.001) and fungal (R^2=26.14%, P<0.001) communities. Constrained and unconstrained analysis of principal coordinates showed distinct separation among samples of different stages, and samples of 3YR stage could be separated from others (Fig. 2d and Additional file 1: Figure S1). Bray-Curtis distances between rhizosphere soils and bulk soils samples also support that the plant developmental stages shape the bacterial and fungal communities, and Bray-Curtis dissimilarities increase with incremental growth (Fig. 2e). These results demonstrate that developmental stages drive succession characteristics in β-diversity of rhizosphere microbiomes.

Developmental stage also affects the microbial composition in rhizosphere of *P. notoginseng* (Fig. 2f-2g, Additional file 1: Figure S2-S3, and Additional file 3-4). Compared to bulk soils, it turns out that bacterial

genera, *Bacillus*, *Paenibacillus* and other genus from the Firmicutes were largely depleted (Fig. 2f and Additional file 5). At the 3YR harvest stage, the root biomass swelled rapidly and accompanied with bacterial enrichment, including *Dyadobacter*, *Dysgonomonas*, *Burkholderia*, *Delftia*, *Flavobacterium*, *Lechevalieria*, and *Hyphomicrobium*. Some fungal genera, e.g. *Cladosporium*, *Epicoccum*, *Leptosphaerulina*, *Phoma*, *Cladophialophora*, *Exophiala*, *Fusarium*, *Plectosphaerella*, and *Ilyonectria*, were also enriched at the 3YR stage (Fig. 2g and Additional file 6). These results reveal that the enrichment and depletion of bacterial and fungal communities occur actively at the 3YR stage.

Response of network structure to *P. notoginseng* developmental stages

All networks obtained follow the power-law distribution (Fig. 3 and Additional file 1:Table S5). Bacterial and fungal networks from rhizosphere soils are much larger than those from bulk soils, as indicated by more nodes and edges in Fig. 3a-3c. The MDS based on graphlet degree distribution distances show that bacterial and fungal communities significantly determine the disparate networks (R=0.97, P<0.001), and the distances among fungal networks constructed from different stages are much larger than that of bacterial networks (Fig. 3a-3b and Additional file 1: Figure S4). The number of nodes and edges in both bacterial and fungal networks constructed from different developmental stages show an increasing and subsequent decreasing trend (Fig. 3c). Modularity and average path length of rhizosphere bacterial and fungal networks decrease more than that of bulk soils (Fig. 3d-3e). As plants grow, modularity and average path length of the bacterial networks decrease slightly, while that of fungal networks increase. OTUs potentially served as keystone taxa in bacterial and fungal networks also changed with the plant growth (Additional file1: Figure S5). These results indicate that the network structure of rhizosphere microbiomes positively reacts to the developmental stages of *P. notoginseng*.

We further explored the robustness of different networks through using the natural connectivity (NC) as the index of graph stability (Fig. 3f). In bacterial graphs, networks obtained from the bulk soils are the most robust, while the network robustness from other stages decrease somewhat. In fungal graphs, networks representing the stages of 2YV and 3YV are the two most robust. Interestingly, compared to the network from bulk soils, the natural connectivity of fungal networks constructed from the rhizosphere soils decreases at a faster rate when sequentially removing nodes in the decreasing sequences of degree or betweenness centralities from the network. These results reveal that the transplantation of *P. notoginseng* reduces the stability of the network.

Core microbiomes related to belowground biomass and saponin content at the harvest stage over spatial scale

To further determine the core rhizosphere microbiomes related to quality of *P. notoginseng* at the 3YR stage (harvest stage), 78 *P. notoginseng* samples were collected from a large-spatial production area. The belowground biomass, saponincontents and rhizospheric microbiomes of *P. notoginseng* show a regional specificity at the harvest stage (Additional file 1: Figure S6-S7 and Additional file 7). Additionally, we identified 639 bacterial OTUs and 310 fungal OTUs as core microbiomes (Fig. 4a-4b, Additional file 1: Figure S7 and Additional file 8). On average, the core bacterial microbiome accounted for 33.27%±9.07%

of the sequences, while the core fungal community accounted for 54.07%±13.74%. The representative phyla include Proteobacteria (43.35%), Acidobacteria (13.81%) and Cyanobacteria (9.82%) in the core bacterial community. At fungal class level, Sordariomycetes (55.04%) and Mortierellomycetes (28.41%) dominate the core community. When a distance-based linear model and forward selection procedure were performed to identify the major environmental variables that shape the core microbial communities, soil pH and OM stand out in both bacterial and fungal communities (Additional file 1: Methods S1, Figure S8 and Table S6).

Random forest analysis showed that both ecological factors and the core microbiome play important roles in the belowground biomass and saponin contents ($P<0.05$) (Fig. 4c). When multivariate regression analysis combined with variation decomposition analysis, the best models also showed that compostion of the core microbiomes were important variables for predicting belowground biomass (bacteria, NMDS2, 4.70%; fungi, NMDS1, 11.53%, NMDS2, 2.78%) and total saponin contents (bacteria, NMDS2, 1.46%; fungi, NMDS1, 2.28%, NMDS2, 8.73%) (Additional file 1: Figure S9 and Table S7). Furthermore, the belowground biomass is strongly correlated with the OTU richness of the core microbiomes ($R^2=0.20$, $P<0.001$ for bacteria; $R^2=0.06$, $P<0.05$ for fungi), and the total saponin contents positively correlated with the OTU richness of the core bacterial microbiomes ($R^2=0.15$, $P<0.001$) (Fig. 4d-4e). Mantel test showed that there were significant correlation between β-diversities of core microbiomes and important indicators of medical value (belowground biomass: bacteria, $r=0.19$, $P<0.001$; fungi, $r=0.34$, $P<0.001$; saponin contents: bacteria, $r=0.11$, $P<0.05$; fungi, $r=0.11$, $P<0.05$; Fig. 4f). These results indicate that OTU richness and β-diversity of the core bacterial and fungal communities are related to the belowground biomass and total saponin contents of *P. notoginseng*.

To relate microbiota to the belowground biomass and saponin contents of *P. notoginseng*, we identified 67 core bacterial genera as the important variables with significance level of $P<0.05$ (Fig. 4g and Additional file 9). The relative abundances of some genera are significantly and positively correlated with belowground biomass ($P<0.05$), such as *Pseudomonas*, *Massilia*, *Sphingobium*, and *Variovorax*. While the abundances of *Nitrospira* and *Comamonas* present a negative correlation ($P<0.05$). Additionally, the total saponin contents exhibits a significant negative correlation with the abundance of some genera, such as *Pseudomonas*, *Sphingobium*, *Massilia*, and *Variovorax*.

Based on RF analysis, we also identified 53 fungal genera (as the important variables with significance level of $P<0.05$) (Fig. 4h and Additional file 9). The relative abundances of some genera are significantly and positively correlated with the belowground biomass ($P<0.05$), such as *Solicoccozyma*, *Phoma*, *Fusidium*, and *Metapochonia*, while the abundance of *Staphylotrichum*, *Phomatospora*, and *Acremonium* exhibit a negative correlation. Three genera are significantly and positively correlated with the total saponin contents ($P<0.05$), namely, *Staphylotrichum*, *Chaetosphaeria*, and *Ganoderma*. But three genera, including *Devriesia*, *Phoma*, and *Metapochonia*, show a significant negative correlation. These results indicate that the core bacterial and fungal genera are related to the belowground biomass and total saponin contents of *P. notoginseng*.

Functions of rhizosphere microbiome related to the belowground biomass and saponin contents in *P. notoginseng*

We obtained a total of 4616 KEGG orthology (KO) functional categories and found that the highly abundant KOs mainly involve several KEGG functional categories of level 2, such as “carbohydrate metabolism”, “amino acid metabolism”, “lipid metabolism”, “metabolism of terpenoids and polyketides”, “xenobiotics biodegradation and metabolism”, “membrane transport” and “signal transduction” (Fig. 5a and Additional file 10-11).

Some functions related to belowground biomass and saponin contents of *P. notoginseng* were obtained in 257 KEGG functional categories of level 3 (Fig. 5a, Additional file 1: Table S8 and Additional file 12). Among them, 36 functions involve in plant-microbe and microbe-microbe interactions, such as bacterial secretion system (ko03070), flagellar assembly (ko02040), bacterial chemotaxis (ko02030), and two-component system (ko02020). Twenty-five microbial functions mediate nutrition acquisition and plant growth, among which galactose metabolism (ko00052), phenylalanine metabolism (ko00360) and beta-alanine metabolism (ko00410) show a positive correlation with belowground biomass (Fig. 5b and Additional file 1: Table S9). Meanwhile positive correlations are also observed between the abundance of fructose and mannose metabolism (ko00051), cysteine and methionine metabolism (ko00270) and total saponin contents. The abundances of functions mediating disease resistance, such as toluene degradation (ko00623), nitrotoluene degradation (ko00633) show a positive correlation with belowground biomass. Meanwhile, the abundances of naphthalene degradation (ko00626) and aminobenzoate degradation (ko00627) are positively correlated with the total saponin contents (Fig. 5b and Additional file 1: Table S9).

Rhizosphere microbiomes driven by *P. notoginseng* developmental stages and core microbiome related to its root growth and saponin contents

Structural equation model (SEM) was constructed to evaluate the effects of environmental factors and developmental stages on rhizosphere microbiomes (Fig. 6a). Month mean temperature (MMT), edaphic factors, and developmental stages were identified as the significant drivers that influence the rhizosphere microbiomes (Fig. 6b). Developmental stages were found to have a significantly direct effect on the PCoA1 (bacteria, 0.76, $P<0.001$; fungi, 0.34, $P<0.001$), PCoA2 (bacteria, 0.19, $P<0.05$; fungi, 0.60, $P<0.001$) and bacterial richness (0.42, $P<0.001$). These data further reveal that *P. notoginseng* developmental stages drive its rhizosphere microbiomes.

Although edaphic factors, climatic factors and rhizosphere microbiomes collectively determine the variability in belowground biomass and total saponin contents of *P. notoginseng* (Fig. 6c), the core bacterial and fungal communities show driving effects. The core bacterial community has a remarkably direct effect on both biomass (PCoA1, 0.29, $P<0.001$) and content (richness, 0.28, $P<0.05$; PCoA4, 0.30, $P<0.05$). The fungal bacterial community also has a significantly and positively direct effect on the contents (richness, 0.15, $P<0.05$; PCoA2, 16, $P<0.05$) but a negative effect on the biomass (PCoA1, -0.27,

P<0.01; PCoA2, -0.18, *P*<0.05). These data further suggest that core rhizosphere microbiomes are related to belowground biomass and total saponin contents.

Discussion

Here, we determined the spatiotemporal dynamics of diversity, composition, and network structures of fungal and bacterial microbiomes during the overall growth stages of *P. notoginseng* and evaluated its rhizosphere microbiomes at a spatial level to determine their core microbiomes and functions related to the belowground biomass and saponin contents. Our results shows that rhizosphere microbiomes are driven by *P. notoginseng* developmental stages, and variations of rhizosphere bacterial communities are also reported during the development stages of *Arabidopsis thaliana* [6]. Compared to bulk soils, the bacterial and fungal diversity exhibits increasing trends in rhizosphere soils of *P. notoginseng*. The α-diversity of rhizobacteria in rhizosphere soils of cotton (*Gossypium hirsutum* L.) were also increased compared with bulk soils [58]. Meanwhile, we noticed that bacterial and fungal diversity increased and then decreased during *P. notoginseng* growth, which is similar to the observations in *P. ginseng* [59] and *Pseudostellaria heterophylla* [60]. These data reveal that succession characteristics of bacterial and fungal diversity are similar as the *P. notoginseng* grew. Our constrained analysis of principal coordinates shows that there is a clear boundary between the bulk and rhizosphere samples. This indicates that compared with the bulk soil community, rhizosphere bacterial and fungal community structures have a host-selective effect, which is consistent with other reports [61, 62]. We observed a sharp increase in Cyanobacteria in the soils of 3YR stage. This may be because Cyanobacteria have a strong ability to colonize the roots of plant and promote plant growth to meet the needs of the rapid root growth at this stage [63]. Putting together, these results indicate that *P. notoginseng* can select a subset of microbes and build up succession characteristics according to its growth needs, and the strength of its rhizosphere effect varies with its growth.

P. notoginseng has a complex network structure in the rhizosphere microbiomes. Compared to the bulk microbiomes, the network is both larger and more complex, a finding similar to the observation in the wild oat (*Avena fatua*) [64]. A large complex network may facilitate more interactions and niche-sharing. However, after transplantation, the modularity and average path length of the bacterial and fungal networks decreased, reflecting the homogeneity of the rhizosphere environment driven by the root exudates [65, 66]. In other words, *P. notoginseng* transplantation reduces the stability of the network. In a previous study, antibiotic treatment in early life also reduced the networks stability of intestinal microbiota [67]. Thus network complexity, a previously undescribed property of the rhizosphere microbiome, appears to be a characteristic of this habitat. The release of exudates relies on the demand of plants, and varies in terms of plant developmental stages, thus leading to the dynamic changes of microbiomes [6, 68]. Plant exudation, such as amino acids, sugars, phenolics, and sugar alcohols, changed with plant developmental stages [69-71]. Sugar exudation could accumulate during Acidobacteria growth [72]. High phenolic acid (-phenol 2,4-di-tert-butylphenol and vanillic acid) concentrations inhibited microbial biomass [73], and phenolics showed a negative correlation with phyla Actinobacteria [74]. Therefore, the rhizosphere microbiome of the 3-year root growth stage is

distinguished from that of the other developmental stages of *P. notoginseng* possibly due to the influence of the root exudates.

P. notoginseng root inflate and grow rapidly at the 3-year root growth stages (harvest stage). Thus, it is particularly valuable to analyze the rhizosphere microbiomes at this stage to understand the microbiome functions of the perennial plant. Our data show that the core bacterial and fungal communities are related to the belowground biomass and total saponin contents of *P. notoginseng.* In foxtail millet, Bacillales, Actinomycetales, Rhizobiales, and Sphigobacteriales were reported to potentially correlate with the high plant productivity . In our study, abundances of some bacterial and fungal genera are significantly and positively correlated with the belowground biomass and total saponin contents of *P. notoginseng*. Many microbes, such as *Bacillus altitudinis* and *Paenibacillus polymyxa*, are beneficial for *P. ginseng* growth, ginsenoside accumulation, and morbidity reduction [76, 77]. The application of *Burkholderia* and *Rhizobium* increased the root growth and ginsenoside contents in *P. ginseng* [22]. These microbes are not only associated with plant growth and secondary metabolites but also can maintain hormonal balance, control root development, promote nutrient acquisition, and prevent diseases of plant, so that they were known as plant beneficial microbes [78, 79]. Therefore, it is important to understand rhizosphere microbes in order to strike a balance between high quality and sustainable production of the herb medicines.

Plant-microbe and microbe-microbe interactions have important effects on rhizosphere microbiomes [80]. This can be evaluated by the correlation between the abundance of functions related to environmental information processing and the belowground biomass. This type of functions commonly includes ABC transporters for exchange of complex molecules, two-component system and bacterial secretion system for intercellular signaling, as well as N metabolism pathway [81-86]. In our study, certain functions such as galactose metabolism, phenylalanine metabolism and beta-alanine metabolism are positively correlated with belowground biomass. Other functions such as fructose and mannose metabolism, cysteine and methionine metabolism are positively correlated with total saponin contents, which also shows positive correlation with the abundances of naphthalene degradation and aminobenzoate degradation. These data suggest that the *P. notoginseng* plant select functionally beneficial microbial communities in the rhizosphere according to its own growth need. Taken together, we determine that core rhizosphere microbiomes associate with belowground biomass and saponin contents of *P. notoginseng*, revealing the adaptability of rhizosphere microbes regulating the important indicators of value in medicinal plants. Our data also demonstrate that climatic factors, edaphic factors, and rhizosphere microbiomes play synergetic roles in promoting belowground biomass and saponin contents of *P. notoginseng*.

Conclusion

Our data show that developmental stage is a significant driving force affecting the rhizosphere microbiomes, and succession characteristics of bacterial and fungal diversity were similar and parabolic patterns during the developmental stages, reflecting the adaptability of the plant microbial communities

to the changes in the plant development. Association analysis at the large-scale reveals that the core rhizosphere microbiome is related to the important medicinal value indicators of the perennial *P. notoginseng*. This work provides a comprehensive understanding in predicting the response of microbial communities and their potential functions in plant growth and accumulation of secondary metabolites. In addition to harness the power of microbiomes to evaluate herbal medicine quality and quantity, our data also provide valuable information in the guidance of microbial breeding for medical plants.

Abbreviations

OTU: Operational taxonomic unit; HPLC: High-performance liquid chromatography; CAP: Constrained analysis of principal coordinate; PCoA: Principal coordinate analysis; RDA: Redundancy analysis; PERMANOVA: Permutational multivariate analysis of variance; SPIEC-EASI: SParse InversE Covariance Estimation for Ecological ASsociation Inference; GDD: Graphlet degree distribution; MDS: Multidimensional scaling; RF: Random forest; SEM: Structural equation model; KO: KEGG orthology.

Declarations

Acknowledgements

We are particularly grateful to Ye Tao for his valuable comments on the data analysis.

Authors' contributions

Conceived and designed the experiments: LLD and SLC. Performed the experiments and analyzed the data: GFW, MZL, GZZ. ZJC, FGW, SJ, JQ, YW, XXM, YQY. Wrote the manuscript: LLD, GFW, MZL, GZZ. All authors read and approved the final manuscript.

Funding

This study was supported by grands from the Beijing Nova Program (No. Z181100006218020), the Fundamental Research Funds for the Central public welfare research institutes (No. ZZ13-AQ-049 and No. ZXKT17049), Major Science and Technology Projects of Yunnan Province (No. 2018ZF011) and National Key R&D Plan (No. 2017YFC1702500).

Availability of data and materials

The raw sequencing data are publicly available in the NCBI Sequence Read Archive (SRA) under the Bioproject number PRJNA559079. R codes on the statistical analyses are available at https://github.com/githubzgz/Panax.notoginseng.

Ethics approval and consent to participate

Not applicable.

Consent for publication

Not applicable.

Competing interests

The authors declare no competing interests.

Author details

[1] Key Laboratory of Beijing for Identification and Safety Evaluation of Chinese Medicine, Institute of Chinese Materia Medica, China Academy of Chinese Medical Sciences, Beijing 100700, China. [2]Institute of Sanqi Research, Wenshan University, Wenshan 663000, China. [3]Wenshan Miaoxiang Notoginseng Technology, Co., Ltd., Wenshan 663000, China. [4]State Key Laboratory of Crop Stress Biology in Arid Areas, College of Life Sciences, Northwest A&F University, Yangling 712100, China.

References

1. Pérez-Jaramillo JE, Mendes R, Raaijmakers JM. Impact of plant domestication on rhizosphere microbiome assembly and functions. Plant Mol Biol. 2016;90:635-44.
2. Liu DF, Sun HJ, Ma HW. Deciphering microbiome related to rusty roots of Panax ginseng and evaluation of antagonists against pathogenic. Front Microbiol. 2019;10:1350.
3. Gomes NCM, Heuer H, Schönfeld J, Costa R, Mendonca-Hagler L, Smalla K. Bacterial diversity of the rhizosphere of maize (*Zea mays*) grown in tropical soil studied by temperature gradient gel electrophoresis. Plant Soil. 2001;232:167-80.
4. Mougel C, Offre P, Ranjard L, Corberand T, Gamalero E, Robin C, et al. Dynamic of the genetic structure of bacterial and fungal communities at different developmental stages of *Medicargo truncatula* Gaertn. cv. Jemalong line J5. New Phytol. 2006;170(1):165-75.
5. Houlden A, Timms-Wilson TM, Day MJ, Bailey MJ. Influence of plant developmental stage on microbial community structure and activity in the rhizosphere of three field crops. FEMS Microbiol Ecol. 2008;65(2):193-201.
6. Chaparro JM, Badri DV, Vivanco JM. Rhizosphere microbiome assemblage is affected by plant development. ISME J. 2014;8(4):790-803.
7. Sugiyama A, Ueda Y, Zushi T, Takase H, Yazaki K. Changes in the bacterial community of soybean rhizospheres during growth in the field. PLoS One. 2014;9(6):

e100709.

8. Tkacz A, Cheema J, Chandra G, Grant A, Poole PS. Stability and succession of the rhizosphere microbiota depends upon plant type and soil composition. ISME J. 2015;

9(11):2349-59.

9. Smalla K, Wieland G, Buchner A, Zock A, Parzy J, Kaiser S, et al. Bulk and rhizosphere soil bacterial communities studied by denaturing gradient gel electrophoresis: plant-dependent enrichment and seasonal shifts revealed. Appl Environ Microbiol. 2001;67(10):4742-51.
10. Kim YJ, Zhang D, Yang DC. Biosynthesis and biotechnological production of ginsenosides. Biotechnol Adv. 2015;33(6 Pt 1):717-35.
11. Dong LL, Xu J, Zhang LJ, Cheng RY, Wei GF, Su H, et al. Rhizospheric microbial communities are driven by *Panax ginseng* at different growth stages and biocontrol bacteria alleviates replanting mortality. Acta Pharm Sin B. 2018;8 (2):272-
12. Zhang HZ, Liu DH, Zhang DK, Wang YH, Li G, Yan GL, et al. Quality assessment of *Panax notoginseng* from different regions through the analysis of marker chemicals, biological potency and ecological factors. PLoS One. 2016;11(10): e0164384.
13. Zhao Q, Wu YN, Fan Q, Han QQ, Paré PW, Xu R, et al. Improved growth and metabolite accumulation in *Codonopsis pilosula* (Franch.) Nannf. by inoculation of *Bacillus amyloliquefaciens* GB03. J Agric Food Chem. 2016;64(43):8103-8.
14. Huang WJ, Long CL, Lam E. Roles of plant-associated microbiota in traditional herbal medicine. Trends Plant Sci. 2018;23(7):559-62.
15. Köberl M, Schmidt R, Ramadan EM, Bauer R, Berg G. The microbiome of medicinal plants: diversity and importance for plant growth, quality and heath. Front Microbiol. 2013;4:400.
16. Sharma SK, Pandit MK. A new species of *Panax* L. (Araliaceae) from Sikkim Himalaya, India. Syst Bot. 2009;34:434-8.
17. Kim DH. Chemical diversity of *Panax ginseng*, *Panax quinquifolium*, and *Panax notoginseng*. J Ginseng Res. 2012;36(1):1-15.
18. Wan JB, Li SP, Chen JM, Wang YT. Chemical characteristics of three medicinal plants of the *Panax* genus determined by HPLC-ELSD. J Sep Sci. 2015;30(6):825- 32.
19. Meng XX, Huang LF, Dong LL, Li XW, Wei FG, Chen ZJ, et al. Analysis of global ecology of *Panax notoginseng* in suitability and quality. Acta Pharm Sin B. 2016;51(9):1483-93.
20. Tan Y, Cui YA, Li HY, Kuang AX, Li XR, Wei YL, et al. Diversity and composition of rhizospheric soil and root endogenous bacteria in *Panax notoginseng* during continuous cropping practices. J Basic Microbiol. 2017;57(4):337-44.
21. Dong LL, Xu J, Feng GQ, Li XW, Chen SL. Soil bacterial and fungal community dynamics in relation to *Panax notoginseng* death rate in a continuous cropping system. Sci Rep. 2016;6:31802.
22. Dong LL, Li Y, Xu J, Yang J, Wei GF, Shen L, et al. Biofertilizers regulate the soil microbial community and enhance *Panax ginseng* yields. Chin Med. 2019;14:20.
23. Cui XM, Chen ZJ, Wang CL, Zeng J. Studies on saponin accumulative in regularities *Panax notoginseng* (Burk) F. H. Chen. Chin J Chin Mater Med. 2001;26 (1):24-5.
24. Heuberger H, Bauer R, Friedl F, Heubl G, Hummelsberger J, Nögel R, et al. Cultivation and breeding of Chinese medicinal plants in Germany. Planta Med. 2010; 76(17):1956-62.

25. Zhang BG, Peng Y, Zhang Z, Liu HT, Qi YD, Liu S, et al. GAP production of TCM herbs in China. Planta Med. 2010;76(17):1948-55.
26. Dong LL, Xu J, Li Y, Fang HL, Niu WH, Li XW, et al. Manipulation of microbial community in the rhizosphere alleviates the replanting issues in *Panax ginseng*. Soil Biol Biochem. 2018;125:64-74.
27. Bao SD. Soil and agricultural chemistry analysis. Beijing: Agriculture Publication; 2000. p. 355-6.
28. Fierer N, Hamady M, Lauber CL, Knight R. The influence of sex, handedness, and washing on the diversity of hand surface bacteria. Proc Natl Acad Sci U S A. 2008;105(46):17994-9.
29. Bolyen E, Rideout JR, Dillon MR, Bokulich NA, Abnet CC, Al-Ghalith GA, et al. Reproducible, interactive, scalable and extensible microbiome data science using QIIME 2. Nat Biotechnol. 2019;37(8):852-7.
30. Edgar RC, Haas BJ, Clemente JC, Quince C, Knight R. UCHIME improves sensitivity and speed of chimera detection. Bioinformatics. 2011;27(16):2194-200.
31. Quast C, Pruesse E, Yilmaz P, Gerken J, Schweer T, Yarza P, et al. The SILVA ribosomal RNA gene database project: improved data processing and web-based tools. Nucleic Acids Res. 2013;41(Database issue):D590-6.
32. Kõljalg U, Nilsson RH, Abarenkov K, Tedersoo L, Taylor AFS, Bahram M, et al. Towards a unified paradigm for sequence-based identification of fungi. Mol Ecol. 2013;22(21):5271-7.
33. Shi WC, Li MC, Wei GS, Tian RM, Li CP, Wang B, et al. The occurrence of potato common scab correlates with the community composition and function of the geocaulosphere soil microbiome. Microbiome. 2019;7(1):14.
34. Wei GF, Dong LL, Yang J, Zhang LJ, Xu J, Yang F, et al. Integrated metabolomic and transcriptomic analyses revealed the distribution of saponins in *Panax notoginseng*. Acta Pharm Sin B. 2018;8(3):458-65.
35. R Core Team. R: A language and environment for statistical computing. R foundation for statistical computing, Vienna, Austria. URL https://www.R-project.org/. 2019.
36. Oksanen J, Blanchet FG, Kindt R, Legendre P, Minchin PR, O'Hara R, et al. Vegan: community ecology package. R package v 22-1, http://CRAN.R-project.org/ package=vegan. 2015.
37. Pohlert T. The pairwise multiple comparison of mean ranks package (PMCMR). R package. http://CRAN.R-project.org/package=PMCMR. 2014.
38. Lozupone C, Knight R. UniFrac: a new phylogenetic method for comparing microbial communities. Appl Environ Microb. 2005;71(12):8228-35.
39. Paradis E, Claude J, Strimmer K. APE: analyses of phylogenetics and evolution in R language. Bioinformatics. 2004;20(2):289-90.
40. Robinson MD, McCarthy DJ, Smyth GK. edgeR: a Bioconductor package for differential expression analysis of digital gene expression data. Bioinformatics. 2010;26(1):139-40.
41. Benjamini Y, Hochberg Y. Controlling the false discovery rate: a practical and powerful approach to multiple testing. J Roy Stat Soc B. 1995;57:289-300.
42. Delgado-Baquerizo M, Oliverio AM, Brewer TE, Benavent-González A, Eldridge DJ, Bardgett RD, et

al. A global atlas of the dominant bacteria found in soil. Science. 2018;359(6373):320-25.
43. Kurtz ZD, Müller CL, Miraldi ER, Littman DR, Blaser MJ, Bonneau RA. Sparse and compositionally robust inference of microbial ecological networks. PLoS Comput Biol. 2015;11(5):e1004226.
44. Liu H, Roeder K, Wasserman L. Stabilityapproach to regularization selection (StARS) for high dimensional graphical models. Adv Neural Inf Process Syst. 2010;24(2):1432-40.
45. Csardi G, Nepusz T. The igraph software package for complex network research. Int J Complex Syst. 2006;1695:1-9.
46. Pons P, Latapy M. Computing communities in large networks using random walks. In proceedings of the 20th international conference on computer and information Sciences. 2005;284-93.
47. Przulj N. Biological network comparison using graphlet degree distribution. Bioinformatics. 2007;23(2):e177-83.
48. Wu J, Mauricio B, Tan YJ, Deng HZ. Natural connectivity of complex networks. Chin Phys Lett. 2010;27(7):078902.
49. Frank E, Harrell Jr. Hmisc: Harrell Miscellaneous. R package version 4.3-0. https://CRAN.R-project.org/package=Hmisc. 2019.
50. Delgado-Baquerizo M, Maestre FT, Reich PB, Jeffries TC, Gaitan JJ, Encinar D, et al. Microbial diversity drives multifunctionality in terrestrial ecosystems. Nat Commun. 2016;7:10541.
51. Laforest-Lapointe I, Paquette A, Messier C, Kembel SW. Leaf bacterial diversity mediates plant diversity and ecosystem function relationships. Nature. 2017;546 (7656):145-7.
52. Jiao S, Xu YQ, Zhang J, Hao X, Lu YH. Core microbiota in agricultural soils and their potential associations with nutrient cycling. mSystems. 2019;4(2):e00313-8.
53. Joshi N, Fass J. Sickle: A sliding-window, adaptive, quality-based trimming tool for fastq files (version 1.33). Software. https://github.com/najoshi/sickle, 2011.
54. Langmesd B, Salzberg SL. Fast gapped-read alignment with Bowtie 2. Nat Methods. 2012;9(4):357-9.
55. Fu LM, Niu BF, Zhu ZW, Wu ST, Li WZ. CD-HIT: accelerated for clustering the next-generation sequencing data. Bioinformatics. 2012;28(23):3150-2.
56. Ye Y, Doak TG. A parsimony approach to biological pathway reconstruction/ inference for genomes and metagenomes. PLoS Comput Biol. 2009;5(8):e1000465.
57. Yves R. Lavaan: An R package for structural equation modeling. J Stat Softw. 2012;48(2):1-36.
58. Qiao Q, Wang F, Zhang J, Chen Y, Zhang CY, Liu GD, et al. The variation in the rhizosphere microbiome of cotton with soil type, genotype and developmental stage. Sci Rep. 2017,7:3940.
59. Xiao CP, Yang LM, Zhang LX, Liu CJ, Han M. Effects of cultivation ages and modes on microbial diversity in the rhizosphere soil of Panax ginseng. J Ginseng Res. 2016;40(1):28-37.
60. Zhao YP, Lin S, Chu LX, Gao JT, Azeem S, Lin WX. Insight into structure dynamics of soil microbiota mediated by the richness of replanted Pseudostellaria heterophylla. Sci Rep. 2016;6:26175.
61. Berg G, Smalla K. Plant species and soil type cooperatively shape the structure and function of microbial communities in the rhizosphere. FEMS Microbiol Ecol. 2009;68 (1):1-13.

62. Uroz S, Buée M, Murat C, Frey-Klett P, Martin F. Pyrosequencing reveals a contrasted bacterial diversity between oak rhizosphere and surrounding soil. Environ Microbiol Rep. 2010;2(2):281-8.
63. Franche C, Lindstrom K, Elmerich C. Nitrogen-fixing bacteria associated with leguminous and non-leguminous plants. Plant Soil. 2009;321:35-59.
64. Shi SJ, Nuccio EE, Shi ZJ, He ZL, Zhou JZ, Firestone MK. The interconnected rhizosphere: high network complexity dominates rhizosphere assemblages. Ecol Lett. 2016;19(8):926-36.
65. Röttjers L, Faust K. From hairballs to hypotheses-biological insights from microbial networks. FEMS Microbiol Rev. 2018;42(6):761-80.
66. Zhou JZ, Deng Y, Luo F, He ZL, Tu QC, Zhi XY. Functional molecular ecological networks. mBio. 2010;1(4):e00169-10.
67. Ruiz VE, Battaglia T, Kurtz ZD, Bijnens L, Ou A, Engstrand I, et al. A single early-in-life macrolide course has lasting effects on murine microbial network topology and immunity. Nat Commun. 2017;8(1):518.
68. Edwards JA, Santos-Medellín CM, Liechty ZS, Nguyen B, Lurie E, Eason S, et al. Compositional shifts in root-associated bacterial and archaeal microbiota track the plant life cycle in field-grown rice. PLoS Biol. 2018;16(2):e2003862.
69. Sasse J, Martinoia E, Northen T. Feed Your Friends: Do plant exudates shape the root microbiome? Trends Plant Sci. 2018;23(1):25-41.
70. Allard-Massicotte R, Tessier L, Lécuyer F, Lakshmanan V, Lucier JF, Garneau D, et al. Bacillus subtilis early colonization of Arabidopsis thaliana roots involves multiple chemotaxis receptors. mBio. 2016;7(6):e01664-16.
71. Badri DV, Chaparro JM, Zhang RF, Shen QR, Vivanco JM. Application of natural blends of phytochemicals derived from the root exudates of Arabidopsis to the soil reveal that phenolic-related compounds predominantly modulate the soil microbiome. J Biol Chem. 2013;288(7):4502-12.
72. Kawasaki A, Donn S, Ryan PR, Mathesius U, Devilla R, Jones A, et al. Microbiome and exudates of the root and rhizosphere of Brachypodium distachyon, a model for wheat. PLoS One. 2016;11(10):e0164533.
73. Qu XH, Wang JG. Effect of amendments with different phenolic acids on soil microbial biomass, activity, and community diversity. Appl Soil Ecol. 2008;39(2): 172-9.
74. Micallef SA, Channer S, Shiaris MP, Colón-Carmona A. Plant age and genotype impact the progression of bacterial community succession in the Arabidopsis rhizosphere. Plant Signal Behav. 2009;4(8):777-80.
75. Jin T, Wang YY, Huang YY, Xu J, Zhang PF, Wang N, et al. Taxonomic structure and functional association of foxtail millet root microbiome. Gigascience. 2017;6(10):1-12.
76. Song XL, Wu H, Yin ZH, Lian ML, Yin CR. Endophytlc bacteria isolated from Panax ginseng improved ginsenoside accumulation in adventitious ginseng root culture. Molecules. 2017;22(6):837.
77. Gao YG, Liu Q, Zang P, Li X, Ji Q, He ZM, et al. An endophytic bacterium isolated from Panax ginseng C.A. Meyer enhances growth, reduces morbidity, and stimulates ginsenoside biosynthesis. Phytochem Lett. 2015;11:132-8.
78. Lemanceau P, Blouin M, Muller D, Moënne-Loccoz Y. Let the core microbiota be functional. Trends

Plant Sci. 2017;22(7):583-95.
79. Verbon EH, Liberman LM. Beneficial microbes affect endogenous mechanisms controlling root development. Trends Plant Sci. 2016;21(3):218-29.
80. Xu J, Zhang YZ, Zhang PF, Trivedi P, Riera N, Wang YY, et al. The structure and function of the global citrus rhizosphere microbiome. Nat Commun. 2018;9(1):4894.
81. Giuliani SE, Frank AM, Corgliano DM, Seifert C, Hauser L, Collart FR.Environment sensing and response mediated by ABC transporters. BMC Genomics. 2011;12 Suppl (Suppl 1):S8.
82. He K, Bauer CE. Chemosensory signaling systems that control bacterial survival. Trends Microbiol. 2014;22(7):389-98.
83. Schenk ST, Stein E, Kogel KH, Schikora A. Arabidopsis growth and defense are modulated by bacterial quorum sensing molecules. Plant Signal Behav. 2012;7(2):178-81.
84. Healy FG, Krasnoff SB, Wach M, Gibson DM, Loria R. Involvement of a cytochrome P450 monooxygenase in thaxtomin a biosynthesis by Streptomyces acidiscabies. J Bacterial. 2002;184(7):2019-29.
85. Kers JA, Wach MJ, KrasnoffSB, Windom J, Cameron KD, Bukhalid RA, et al. Nitration of a peptide phytotoxin by bacterial nitric oxide synthase. Nature. 2004;429
(6987):79-82.
86. Barry SM, Kers JA, Johnson EG, Song LJ, Aston PR, Patel B, et al. Cytochrome P450-catalyzed L-tryptophan nitration in thaxtomin phytotoxin biosynthesis. Nat Chem Biol. 2012;8(10):814-6.

Figures

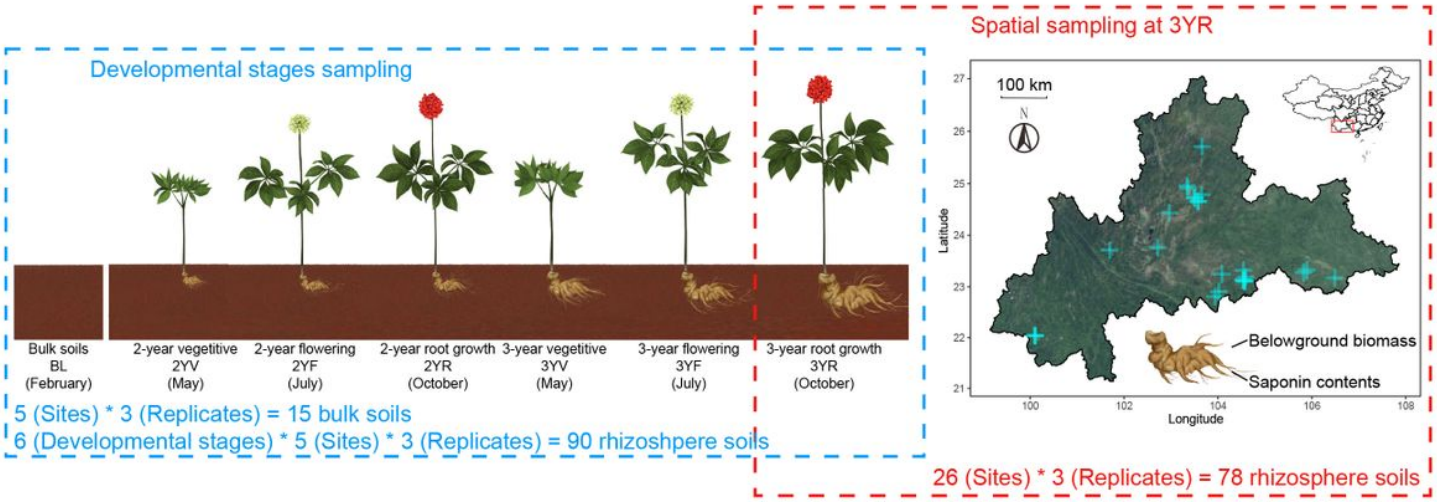

Figure 1

The model of experimental samples collection. Blue and red boxes represent models of developmental stages and spatial sampling experiments, respectively. Bulk soils were collected from farmlands before P. notoginseng transplanting. Rhizosphere soil samples were collected from P. notoginseng plants.

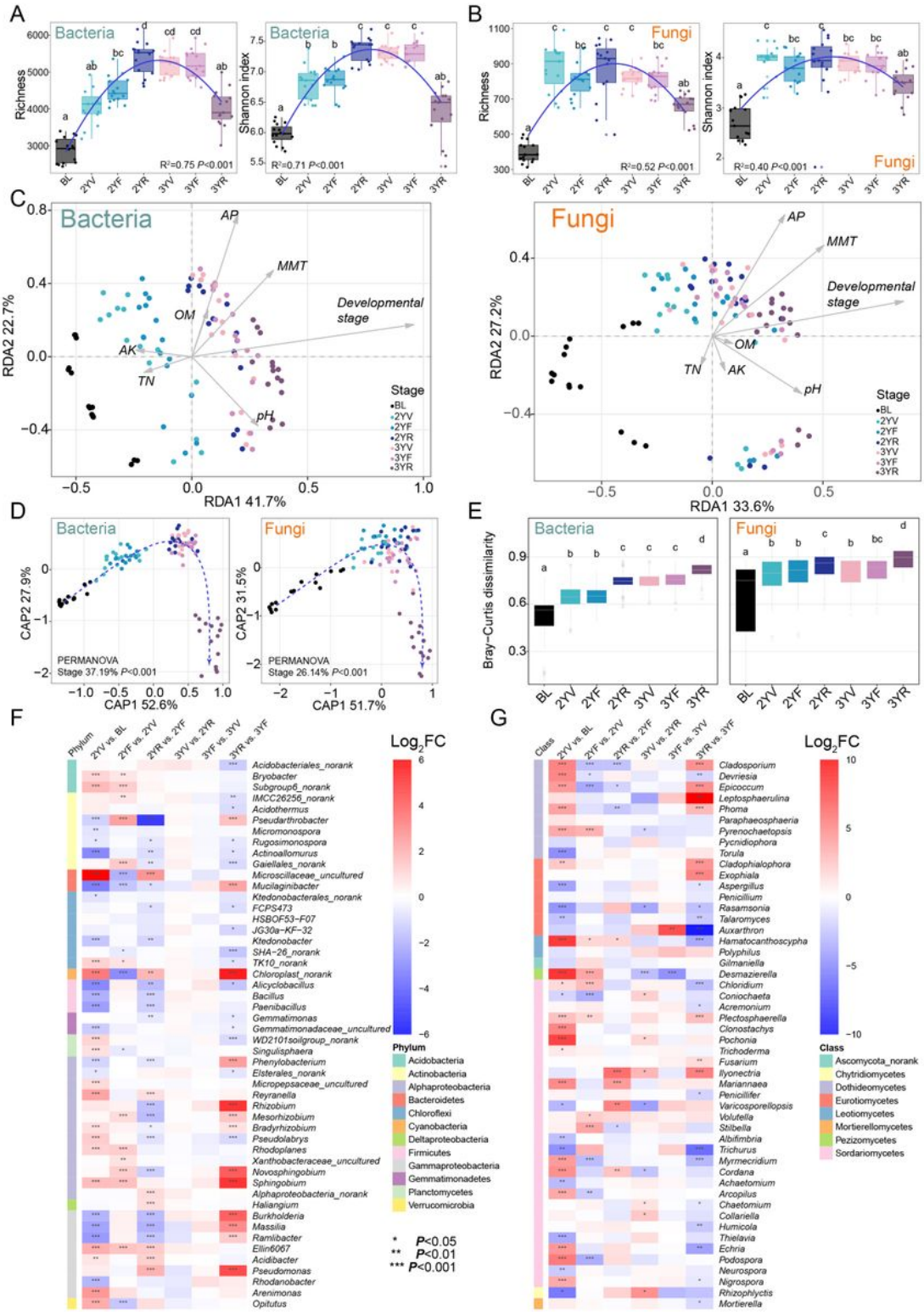

Figure 2

Changes in diversity and composition of bacterial and fungal communities across developmental stages of P. notoginseng. Bacterial (a) and fungal (b) α-diversity at different growth stages represented by OTU richness and Shannon index. (c) The effects of external factors on microbial communities based on redundancy analysis (RDA). MMT: month mean temperature; AK: available potassium; OM: organic matter; AP: available phosphate; TN, total nitrogen. (d) Variation of bacterial and fungal communities

constrained to developmental stages based on principal coordinates analysis (CAP). (e) Bray-Curtis distances between bulk soils and rhizosphere soils of other stages. The enrichment and depletion of bacterial (f) and fungal (g) genera with average relative abundance of top 50. Color represent log transformed fold change. Different letters denote for significant between compared groups (P < 0.05).

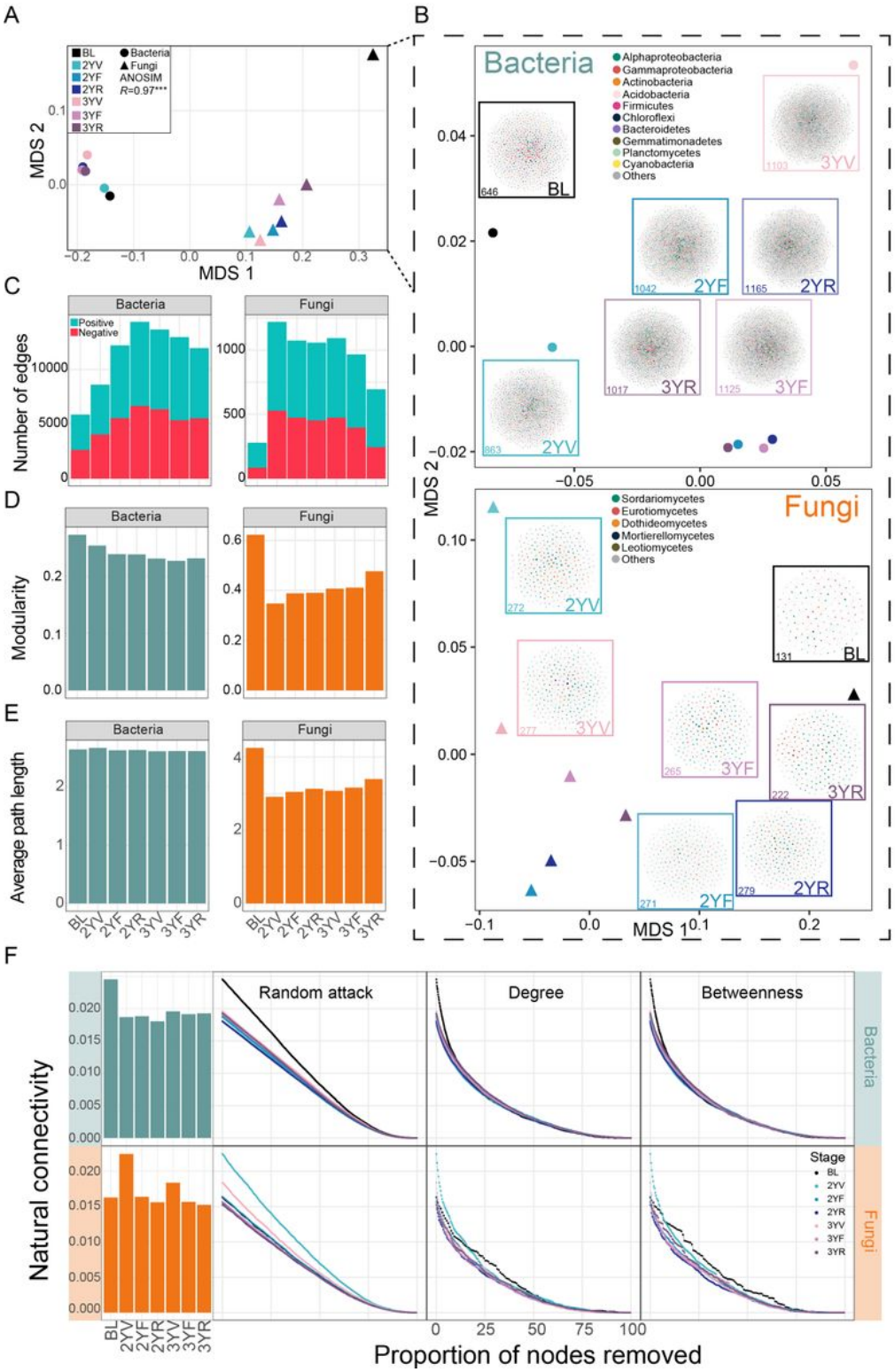

Figure 3

Changes in interaction patterns of bacterial and fungal communities across developmental stages of P. notoginseng. Combined (a) and within domain (b) similarity analysis of bacterial and fungal networks using MDS based on graphlet degree distribution. The number in the left bottom of small squares represent the number of nodes. Nodes are colored at phylum and class level for bacterial and fungal networks, respectively. (c) Number of edges of networks. Red and green represent negative and positive links, respectively. Modularity (d) and (e) average path length of networks. (f) The robustness of networks represented by natural connectivity. Three types of attack robustness, including removing nodes from networks randomly, sequentially in the order of degree and betweenness are shown in line pots.

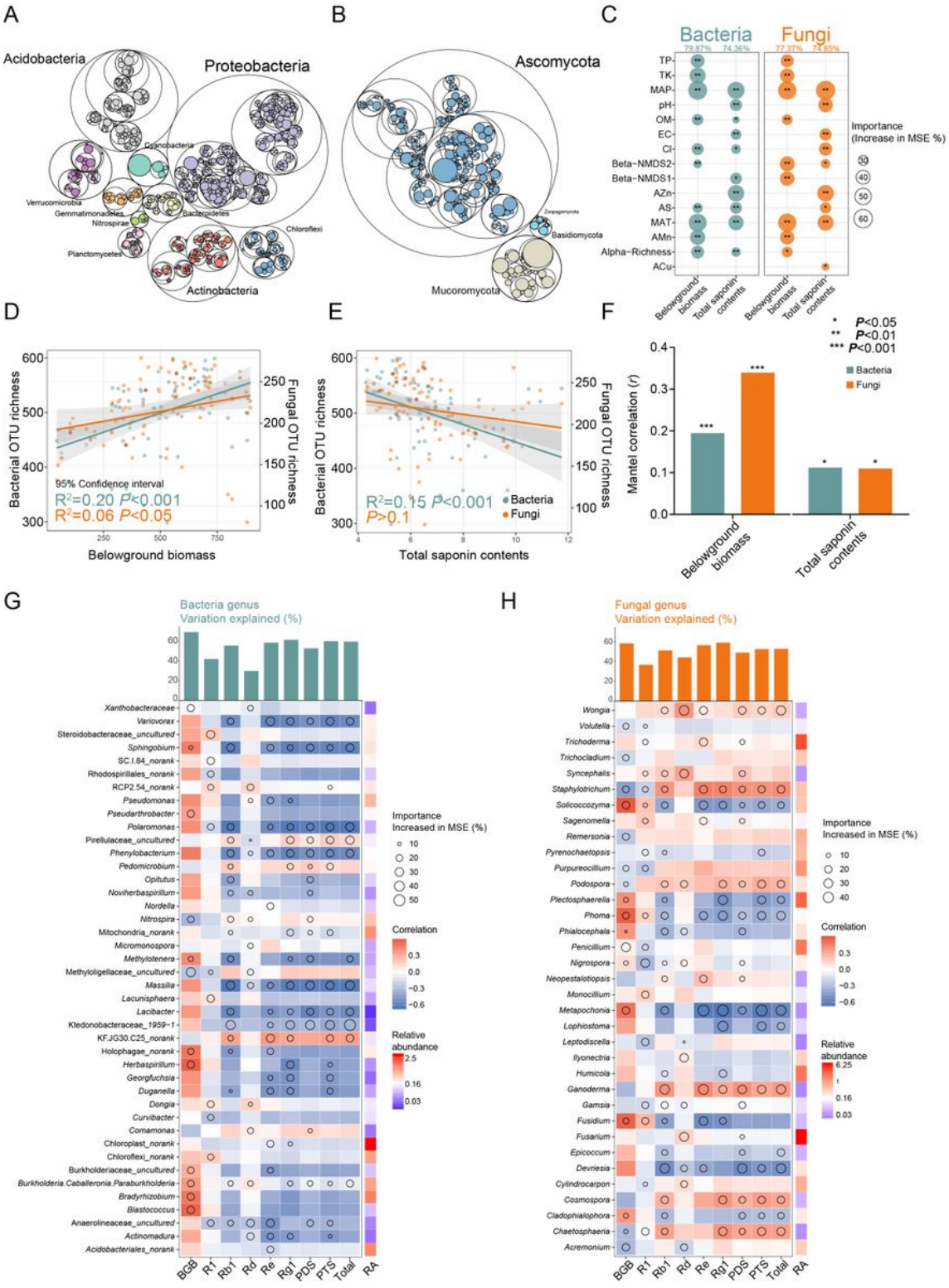

Figure 4

Contributions of the core microbiota to belowground biomass and saponins contents in P. notoginseng. The abundance of core bacterial (a) and fungal (b) communities. (c) Mean predictor importance of environmental factors and core microbiomes for belowground biomass and total saponins contents. Numbers above plots represent variance explained by the model. TP: total phosphate; TK: total potassium; MAP: mean annual precipitation; OM: organic matter; EC: electric conductivity; AZn: available

zinc; AS: available sulfur; MAT: mean annual temperature; AMn: available manganese; ACu: available copper; Alpha-Richness: the OTU richness of core bacterial or fungal microbiomes; Beta-NMDS1 & Beta-NMDS2: the two axes of nonmetric multidimensional scaling analysis of core bacterial and fungal microbiomes. The linear relationship between OTU of core bacterial and fungal microbiomes and belowground biomass (d) and total saponins contents (e). Correlations between β-diversity of core microbiomes and medical value indicators estimated by Mantel test (f). Core bacterial (g) and fungal (h) genus related to belowground biomass and saponins contents based on random forest; The top 10 most important and significant (P<0.05) genus for each model are shown. Colors represent spearman correlations. BGB, PDS, PTS, Total, and RA represent belowground biomass, contents of 20(S)-protopanaxadiol saponins (including Rd and Rb1), contents of 20(S)-protopanaxatriol saponins (including R1, Rg1 and Re), total saponins contents, and relative abundance, respectively.

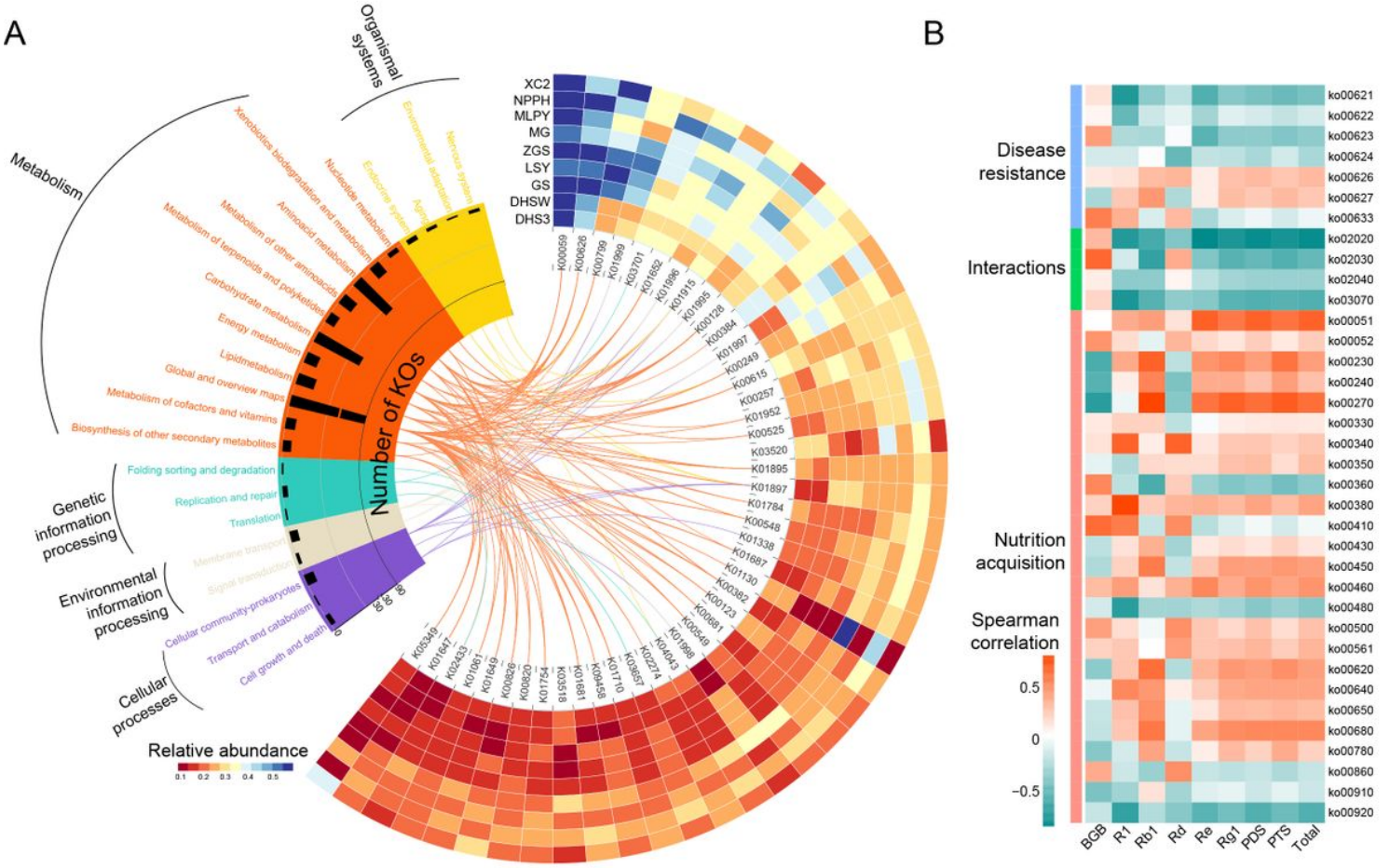

Figure 5

Profiles of functions and their correlations with belowground biomass and saponins contents. (a) Abundance distribution of KO functional categories with relative abundance > 0.20%. (b) Spearman correlation analysis among functions in level 3 with related to belowground biomass and saponins contents. BGB, PDS, PTS and Total represent belowground biomass, total contents of 20(S)-protopanaxadiol saponins (including Rd and Rb1), total contents of 20(S)-protopanaxatriol saponins (including R1, Rg1 and Re), total contents of PDS and PTS, respectively.

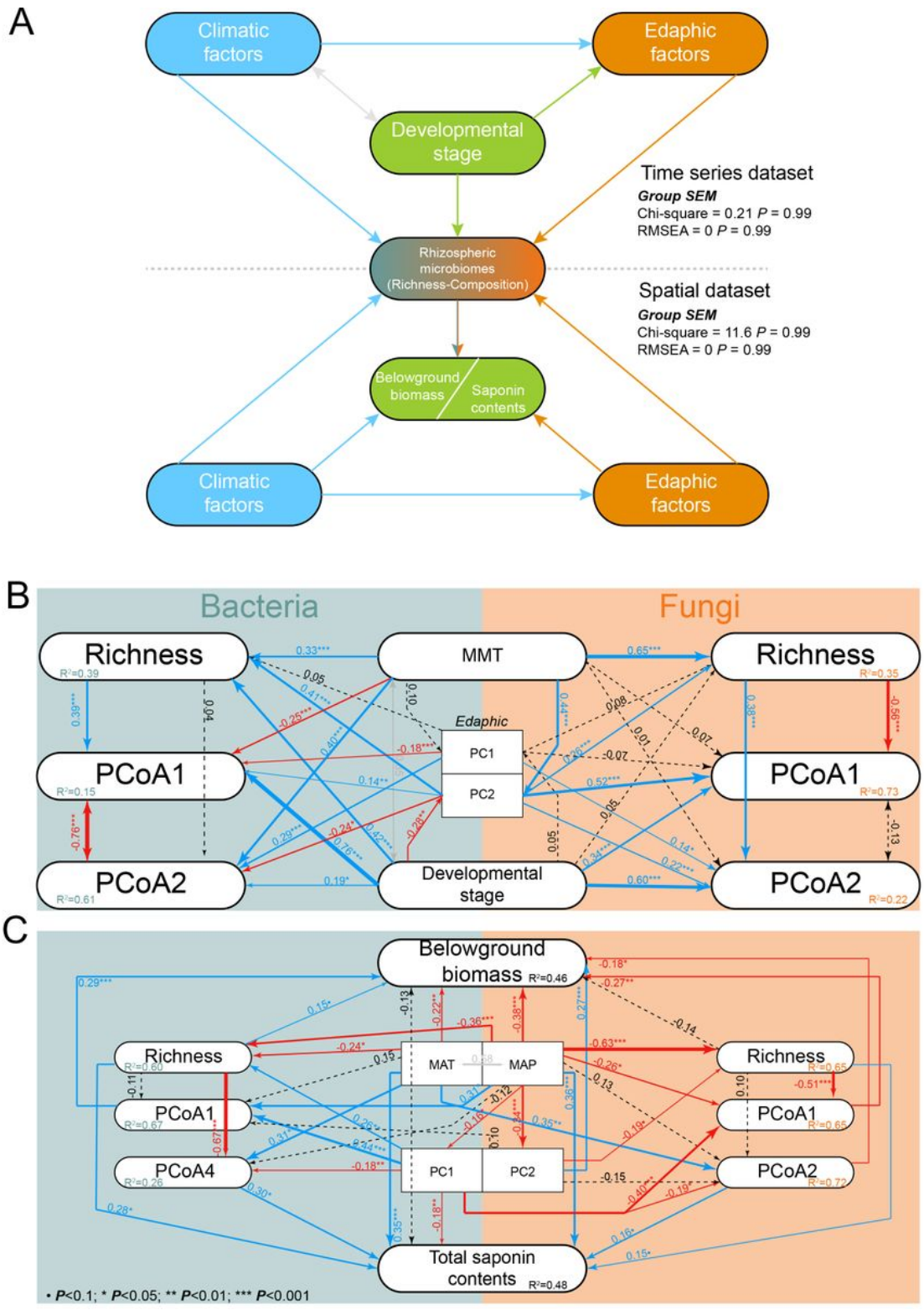

Figure 6

Structural equation models (SEMs) of time series dataset and spatial dataset. (a) Schematic diagram of two SEMs and corresponding statistics. (b) Effects of climatic factors, edaphic factors, and developmental stages on rhizosphere communities in developmental stages sampling dataset. (c) Effects of climatic factors, edaphic factors, and rhizosphere communities on belowground biomass and total saponins contents in spatial sampling dataset. PC1 and PC2 represent the first and second axes of

principal coordinate analysis (PCA) of edaphic factors; PCoA1, PCoA2 and PCoA4 represent the first, second and fourth axes of principal coordinate analysis (PCoA) based on Bray-Curtis distances among bacterial or fungal communities; Richness: OTU richness of bacterial and fungal communities. MMT: month mean temperature. MAT: mean annual temperature. MAP: mean annual precipitation. Solid lines represent significant ($P<0.1$) path coefficients (blue: positive; red: negative), while dotted lines represent path with $P \geq 0.1$. Gray line represents correlation between independent variables. R2 represent variance explained by the model.

Supplementary Files

This is a list of supplementary files associated with this preprint. Click to download.

- Additionalfile12.xls
- Additionalfile11.xls
- Additionalfile10.xls
- Additionalfile9.xls
- Additionalfile8.xls
- Additionalfile7.xls
- Additionalfile6.xls
- Additionalfile5.xls
- Additionalfile4.xls
- Additionalfile3.xls
- Additionalfile2.xls
- Additionalfile1.pdf